Environ. Res. Lett. **6** (2011) 024023 (6pp) doi:10.1088/1748-9326/6/2/024023

Estimation of chlorophyll-a concentration in productive turbid waters using a Hyperspectral Imager for the Coastal Ocean—the Azov Sea case study

Anatoly A Gitelson[1,4], Bo-Cai Gao[2], Rong-Rong Li[2], Sergey Berdnikov[3] and Vladislav Saprygin[3]

[1] The Center for Advanced Land Management Information Technologies (CALMIT), School of Natural Resources, University of Nebraska-Lincoln, Lincoln, NE 68583, USA
[2] Remote Sensing Division, Naval Research Laboratory, Code 7230, Washington, DC 20375, USA
[3] The Southern Scientific Center of the Russian Academy of Sciences, Rostov-on-Don, 344 000, Russia

E-mail: agitelson2@unl.edu

Received 8 March 2011
Accepted for publication 10 June 2011
Published 30 June 2011
Online at stacks.iop.org/ERL/6/024023

Abstract
We present here the results of chlorophyll-a (chl-a) concentration estimation using the red and near infrared (NIR) spectral bands of a Hyperspectral Imager for the Coastal Ocean (HICO) in productive turbid waters of the Azov Sea, Russia. During the data collection campaign in the summer of 2010 in Taganrog Bay and the Azov Sea, water samples were collected and concentrations of chl-a were measured analytically. The NIR–red models were tuned to optimize the spectral band selections and chl-a concentrations were retrieved from HICO data. The NIR–red three-band model with HICO-retrieved reflectances at wavelengths 684, 700, and 720 nm explained more than 85% of chl-a concentration variation in the range from 19.67 to 93.14 mg m^{-3} and was able to estimate chl-a with root mean square error below 10 mg m^{-3}. The results indicate the high potential of HICO data to estimate chl-a concentration in turbid productive (Case II) waters in real-time, which will be of immense value to scientists, natural resource managers, and decision makers involved in managing the inland and coastal aquatic ecosystems.

Keywords: chlorophyll-a, HICO, NIR-red algorithm, remote sensing, turbid productive waters

1. Introduction

Remote estimation of the concentrations of water constituents is based on the relationship between the remote sensing reflectance, $R_{rs}(\lambda)$, and the inherent optical properties, backscattering coefficient, $b_b(\lambda)$, and absorption coefficient, $a(\lambda)$ (Gordon *et al* 1975):

$$R_{rs}(\lambda) \propto \frac{b_b(\lambda)}{a(\lambda) + b_b(\lambda)} \quad (1)$$

where $a(\lambda)$ is the sum of the absorption coefficients of phytoplankton pigments, a_{pigm}, colored dissolved organic matter, a_{CDOM}, non-algal particles, a_{NAP}, and pure water, a_{water} (e.g. Gordon *et al* 1988). To retrieve the chl-a concentration from spectral reflectance, one has to isolate the chl-a absorption

[4] Author to whom any correspondence should be addressed.

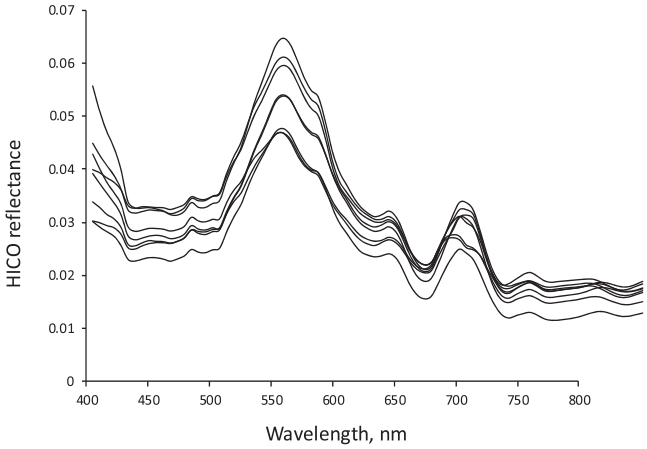

Figure 1. Reflectance spectra acquired by HICO on 13 July 2010.

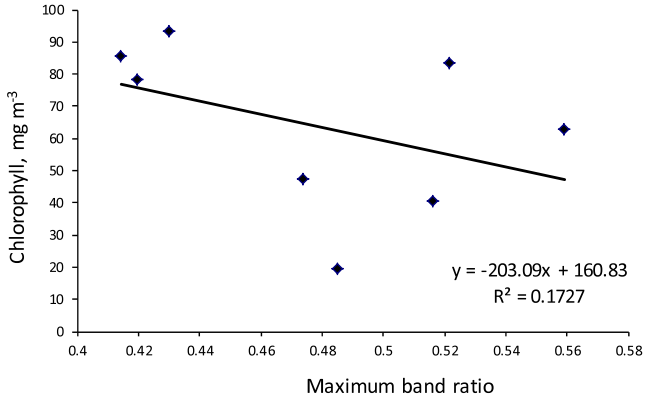

Figure 2. Maximum band ratio algorithm (e.g. O'Reilly *et al* 1998) applied to estimate chl-a concentration.

coefficient. In open ocean waters chl-a is derived using the blue and green spectral regions (e.g. Gordon and Morel 1983). However, in the turbid productive case 2 waters (Morel and Prieur 1977) these spectral regions cannot be used to estimate chl-a because of the overlapping, uncorrelated absorptions by CDOM and NAP, which are much larger in these waters (e.g. Gitelson 1992, Gons 1999, Dall'Olmo and Gitelson 2005a, 2005b).

Algorithms developed for estimating chl-a in turbid productive waters are based on the properties of the reflectance peak near 700 nm (e.g. Vasilkov and Kopelevich 1982, Gitelson *et al* 1985, Stumpf and Tyler 1988, Gitelson 1992, Gons 1999, Gower *et al* 1999). Recently, Dall'Olmo *et al* (2003), Dall'Olmo and Gitelson (2005a) provided evidence that a three-band reflectance model, originally developed for estimating pigment contents in terrestrial vegetation (Gitelson *et al* 2003, 2005), could also be used to assess chl-a in turbid productive waters. The model relates pigment concentration C_{pigm} to reflectance $R(\lambda_i)$ in three spectral bands λ_i (Gitelson *et al* 2003):

$$C_{\text{pigm}} \propto [R^{-1}(\lambda_1) - R^{-1}(\lambda_2)] \times R(\lambda_3). \quad (2)$$

It was shown that for estimating chl-a concentration, λ_1 should be in the red range around 670 nm, λ_2 in the range around 710 nm and λ_3 in the NIR range around 750 nm (Dall'Olmo and Gitelson 2005a, 2006, Gitelson *et al* 2007, 2008).

This study focuses on assessing the potential of the (a) NIR–red models to estimate chl-a concentrations in turbid productive waters using Hyperspectral Imager for the Coastal Ocean (HICO) data and (b) HICO hyperspectral data for estimating other phytoplankton pigments.

2. Data and methods

HICO is the first hyperspectral imager specifically made for environmental characterization of the coastal ocean from space. HICO images one scene per 90 min orbit, with each scene spanning an area approximately 42 km wide and 190 km long, large enough to capture the scale of coastal ocean dynamics. Each pixel is a 95 m square, with 88 spectral channels covering the range from 400 to 900 nm. This includes visible light (400–700 nm), which penetrates the water and provides information on water properties and bottom reflectance, and shortwave infrared radiation (700–900 nm), which is used to correct for atmospheric aerosols and surface reflectance (Lucke *et al* 2011, Corson and Davis 2011).

The field data collection campaign was undertaken on 13–15 July 2010 over Taganrog Bay and the Azov Sea by the crew at the Southern Scientific Center of the Russian Academy of Sciences, Rostov-on-Don, Russia. Water samples were collected at eight stations, filtered through Whatman GF/F glass filters on board a vessel, and analyzed for chl-a. The chl-a concentration was measured through extraction in 90% acetone.

One set of hyperspectral imaging data was acquired with the HICO instrument on board the International Space Station over the Azov Sea on 13 July, the first day of the field campaign. Water leaving reflectances were retrieved from the HICO radiance data using the hyperspectral atmosphere correction algorithm (ATREM) of Gao and Davis (1997). Another set of hyperspectral imaging data was acquired on 1 August, but no field data were taken at that time.

3. Results and discussion

The minimum, maximum, median, and mean *in situ* chl-a concentrations of the eight stations were 19.67 mg m^{-3}, 93.14 mg m^{-3}, 63.86 mg m^{-3}, and 70.6 mg m^{-3} respectively. The water leaving reflectance spectra (figure 1) were quite similar in magnitude and shape to the reflectance spectra collected in turbid productive waters (Lee *et al* 1994, Dall'Olmo and Gitelson 2005a, Schalles 2006, Gitelson *et al* 2008). The maximum band ratio, calculated as the maximum of three reflectance (R) band ratios at wavelengths 443, 490, 520 and 565 nm ($R443/R565$, $R490/R565$, $R520/R565$), used for estimating chl-a concentrations in case I ocean waters (e.g. O'Reilly *et al* 1998, 2000), is poorly related to the chl-a concentrations (figure 2) due to multiple factors that contribute to the reflectance patterns in the blue and green spectral regions. These include absorption by CDOM and non-algal particles as well as backscattering by particulate matter.

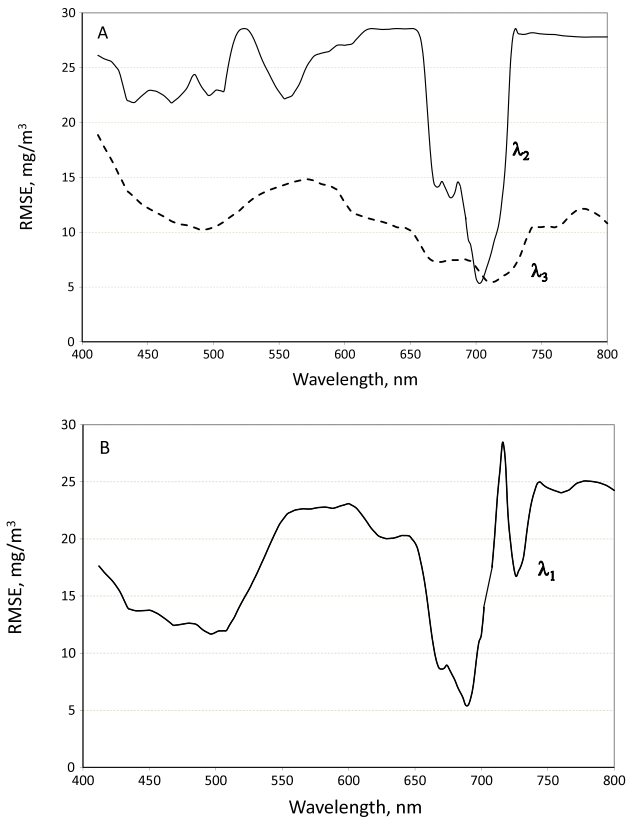

Figure 3. RMSE of chl-a estimation: tuning spectral bands of the three-band model (equation (2)) for λ_2 and λ_3 (A) and λ_1 (B).

Thus, this maximum band ratio algorithm was inadequate for accurate estimation of chl-a concentrations in these case 2 waters (Gitelson 1992, Darecki and Stramski 2004, Dall'Olmo and Gitelson 2005a).

The contiguous HICO spectral data allow the detection of fine spectral features, which include (figure 1): (a) chl-a and carotenoids absorption in the range 430–520 nm, (b) peak of reflectance in the green region around 560 nm due to minimal absorption by all pigments, (c) small trough of reflectance around 570 nm due to phycoerythrin absorption, (d) trough near 630 nm caused by phycocyanin (PC) absorption, (e) pronounced minimum due to red chl-a absorption, and (g) peak around 700 nm caused by minimum of combined absorption of algae and water.

The fine spectral resolution of HICO data permits the tuning of spectral bands of the three-band model (equation (2)) in accord with the optical properties of waters studied. We adapted an optimization procedure based on minimizing the root mean square error (RMSE) of chl-a estimates (Dall'Olmo and Gitelson 2005a, Gitelson *et al* 2008). The procedure optimizes the wavelengths used in the model (equation (2)) by initially setting $\lambda_1 = 665$ nm (red chl-a absorption maximum) and $\lambda_3 = 730$ nm (reflectance at this wavelength is not affected by pigment absorption and is governed by scattering from all particulate matter). Then we regressed the model $[R_{rs}(665)^{-1} - R_{rs}(\lambda_2)^{-1}] \times R_{rs}(730)$ against the measured chl-a concentration to determine the optimal position of λ_2. The minimal RMSE of the chl-a estimation was at 700 nm (figure 3(A)). In the second iteration, λ_2 was set to 700 nm

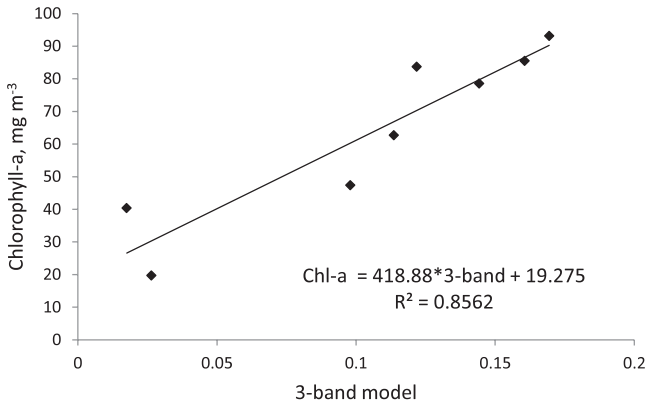

Figure 4. Chl-a estimates by the three-band model (equation (2)) with $\lambda_1 = 684$ nm, $\lambda_2 = 700$ nm, and $\lambda_3 = 720$ nm plotted versus measured chl-a.

and then the model $[R_{rs}(665)^{-1} - R_{rs}(700)^{-1}] \times R_{rs}(\lambda_3)$ was regressed against the measured chl-a concentrations for determination of λ_3. The minimal RMSE was found in the range of λ_3 around 710–720 nm (figure 3(A)). In the final iteration, λ_3 was set to 720 nm and λ_1 was optimized by regressing the model $[R_{rs}(\lambda_1)^{-1} - R_{rs}(700)^{-1}] \times R_{rs}(720)$ against the measured chl-a concentrations. Optimal λ_1 was found at 684 nm (figure 3(B)). Thus, the model for chl-a estimation was optimized in the form:

$$\text{chl-a} = 418.88\{[R_{rs}(684)^{-1} - R_{rs}(700)^{-1}]R_{rs}(720)\} + 19.275. \quad (3)$$

The results of optimization show that the spectral bands of the observing system should be quite narrow to provide an estimation of chl-a concentration with RMSE below 5 mg m^{-3} (figure 3).

Estimates of chl-a concentration by the three-band model (equation (3)) are presented in figure 4. The NIR–red model that used HICO-retrieved reflectances explained more than 85% of the chl-a variation and enabled estimation of chl-a ranging between 17 and 93.14 mg m^{-3} with RMSE below 10 mg m^{-3}. A good match between estimates and the measured chl-a illustrates the great potential of hyperspectral data for monitoring chl-a in coastal and inland waters.

The left-hand panel in figure 5 shows a true color image (red: 640 nm; green: 550 nm; blue: 470 nm) processed from the HICO data acquired over the Sea of Azov on 13 July 2010. The highly productive water areas appear green. The right panel in figure 5 shows the distribution of chl-a concentrations derived from the HICO data set using equation (3). The land areas as well as the areas covered by thin clouds and cloud shadows are masked in gray color. Detailed chlorophyll spatial distribution patterns are clearly seen in this image.

The results presented here as well as from proximal sensing (Dall'Olmo and Gitelson 2005a, Gitelson *et al* 2008, 2009, Yacobi *et al* 2011, Gitelson *et al* 2011) and satellite remote sensing (Moses *et al* 2009a, 2009b, Gitelson *et al* 2011) illustrate the potential of the NIR–red models to estimate chl-a concentration in turbid productive waters. However, it is not clear whether the regression shown in figure 4 is valid for chl-a values below 40 mg m^{-3} as only a few stations

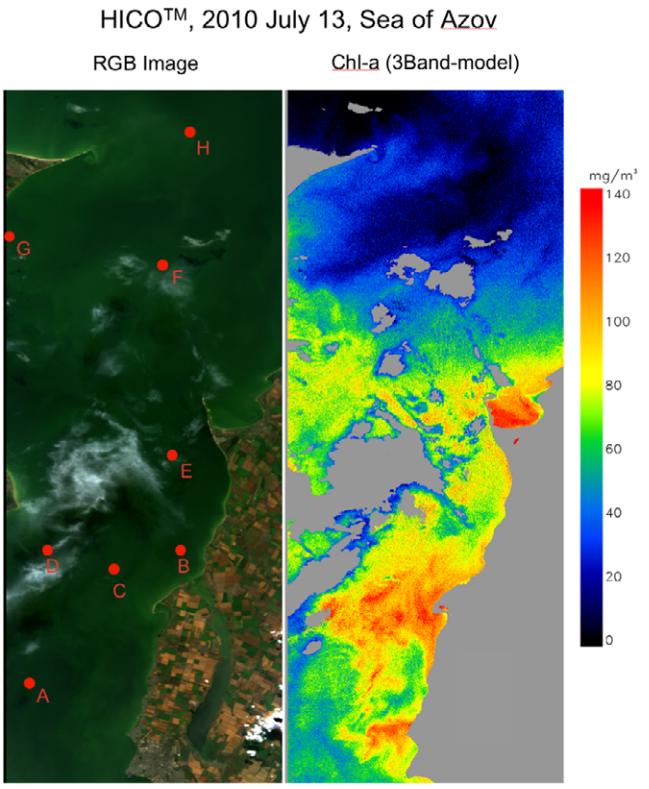

Figure 5. A true color image (left-hand panel) and a chl-a concentration distribution (right panel) obtained from a HICO data set acquired over the Sea of Azov on 13 July 2010. In RGB image points of sampling are presented. Chl-a concentration at stations (in mg m^{-3}): A—62, B—85, C—93, D—83, E—78, F—40, G—47, and H—19.5.

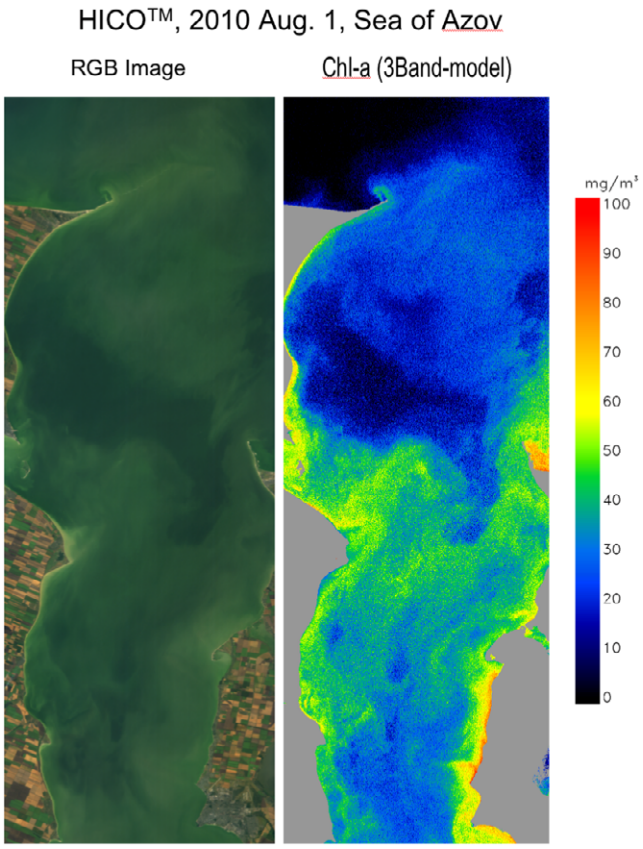

Figure 6. A true color image (left-hand panel) and a chlorophyll-a concentration distribution (right-hand panel) retrieved from a HICO data set acquired over the Sea of Azov on 1 August 2010.

with chl-a concentration were sampled and there is a quite wide scattering of points from the best-fit function. The relationship between chl-a concentrations, ranged from 0.65 to 48 mg m^{-3}, and MERIS (MEdium Resolution Imaging Spectrometer) NIR–red models were linear and very close with R^2 above 0.95 (Moses *et al* 2009a, 2009b, Matishov *et al* 2010). Although the accuracy of chl-a concentration below 40 mg m^{-3} was not an issue in previous studies using MERIS data, this has to be addressed further. Except for the results obtained from a limited dataset in this study and by Moses *et al* (2009a, 2009b) and Matishov *et al* (2010), it has not yet been possible to consistently calibrate this relationship so as to quantitatively estimate the chl-a concentration using satellite data. Some factors make it difficult to develop reliable calibration equations when satellite data are used. Firstly, a successful correction for atmospheric effects and an accurate retrieval of surface reflectance are crucial to the success of the NIR–red model. It is especially important for the retrieval of low-to-moderate chl-a concentration. Without actual *in situ* measurements of water leaving radiance taken at the time of satellite overpass, it is not possible to assess the precision of the atmospheric correction procedure. Secondly, a satellite captures its entire swath within a matter of a few seconds whereas it takes several hours or days to collect *in situ* data. With the inland, estuarine, and coastal waters being very dynamic, during the time between satellite overpass and *in situ* data acquisition the water might have undergone considerable changes in its optical characteristics and constituent concentrations. Finally, the spatial heterogeneity of chl-a distribution in the water body might be such that the point *in situ* sampling may not exactly represent the satellite pixel area (e.g. figure 8 in Moses *et al* (2009a) showing wide spatial variability of chl-a concentration in the Azov Sea). Thus, the model needs to be calibrated and validated with a larger data set including low-to-moderate chl-a concentration.

Despite the fact that the NIR–red model (equation (3) and figure 4) has not yet been validated, we use equation (3) to derive the chl-a concentration from the HICO image acquired on 1 August. The goal was to illustrate the chl-a distribution in the Azov Sea 18 days after the first image was taken. Figure 6 presents a true color image (left-hand panel) and chl-a distribution (right-hand panel) retrieved from a HICO data set acquired on 1 August 2010. Comparing the chl-a distributions in figures 5 and 6, it is seen how drastically different the spatial distribution patterns are in a short time interval of only 18 days. Such a high density of phytoplankton, as can be seen in the map retrieved from the image of 13 July, was unique and disappeared due to a strong northeast wind, a sharp decrease in water depth, a re-suspension of bottom material, and decreased water transparency and, thus, depth of light penetration. The comparison shows how dynamic chl-a concentrations are. Such dynamic behavior of phytoplankton

in estuarine and coastal waters requires frequent monitoring, allowing scientists and decision makers to better understand spatial and temporal phytoplankton patterns and decrease uncertainties in estimating carbon budget in these productive waters.

In addition to increasing the accuracy of the chl-a concentration estimation using narrow spectral bands (see figure 3 for λ_1 and λ_2), HICO hyperspectral data may also be very helpful in quantifying the concentration of other phytoplankton pigments such as phycoerythrin, phycocyanin (PC), and chlorophylls-b and -c. Figure 7 presents the median spectrum of reflectance obtained by HICO over the Azov Sea (panel (A)) and the first derivative of reflectance with respect to wavelength (panel (B)). It shows that many fine absorption features of different phytoplankton pigments (Bidigare *et al* 1990) can be clearly detected by HICO; this allows for the development and testing of the techniques for their retrieval. Multi-band instruments, such as MODIS or MERIS (the bands of MERIS are shown in figure 7(A)) will not be able to capture the fine spectral absorption features. As is seen in figure 7, a slight trough around 570 nm due to phycoerythrin absorption (point a) yields a pronounced minimum in the first derivative spectra (figure 7(B)). To quantify phycoerythrin concentration, one needs hyperspectral resolution data at wavelengths surrounding this trough. The area under a continuum line between 560 and 580 nm may be a good proxy of phycoerythrin absorption.

Minimum reflectance around 630 nm (point b in figure 7(A)) is caused by PC and other accessory pigments, such as chlorophyll-c and chlorophyll-b. Simis *et al* (2005) proposed quantification of PC concentration using reflectance at 625 nm, attributed the absorption signal at 625 nm to PC, as well as attributing reflectances at 670 nm (point c) to chl-a absorption and around 700 nm to the minimum of the combined absorption of phytoplankton pigments and water. The initial tests have shown that the algorithm generally provides overestimations of the PC, except when high PC concentrations associated with massive blue-green algae blooms were observed (Simis *et al* 2007). The authors conclude that correction for the absorption around 625 nm by other accessory pigments, such as chlorophyll-c and chlorophyll-b, is needed to yield more realistic PC assessments in inland and coastal waters. However, only hyperspectral instruments, such as HICO, bring such opportunities.

4. Conclusions

This paper demonstrates clearly the value of a hyperspectral instrument in providing a fine resolution of the water leaving reflectance due to various photosynthetic pigments and dissolved and particulate matter. The results presented here illustrate the high potential of the Hyperspectral Imager for the Coastal Ocean using the NIR–red model to accurately estimate chl-a concentration in turbid productive waters. To the best of our knowledge, this is the first time that this model has been used for chl-a retrieval from HICO data. However, the models need to be calibrated and validated with a larger dataset. Challenges still remain in calibrating the model for their universal application to HICO data as well as quantification of other accessory pigments, such as phycoerythrin, phycocyanin, chlorophyll-b and chlorophyll-c. Provided these algorithms can be effectively tested, robustly calibrated algorithms can be developed for applying the NIR–red models to hyperspectral satellite data for real-time quantitative measurements of phytoplankton pigment concentration, which will greatly benefit scientists and natural resource managers in making informed decisions on managing the inland, coastal, and estuarine ecosystems.

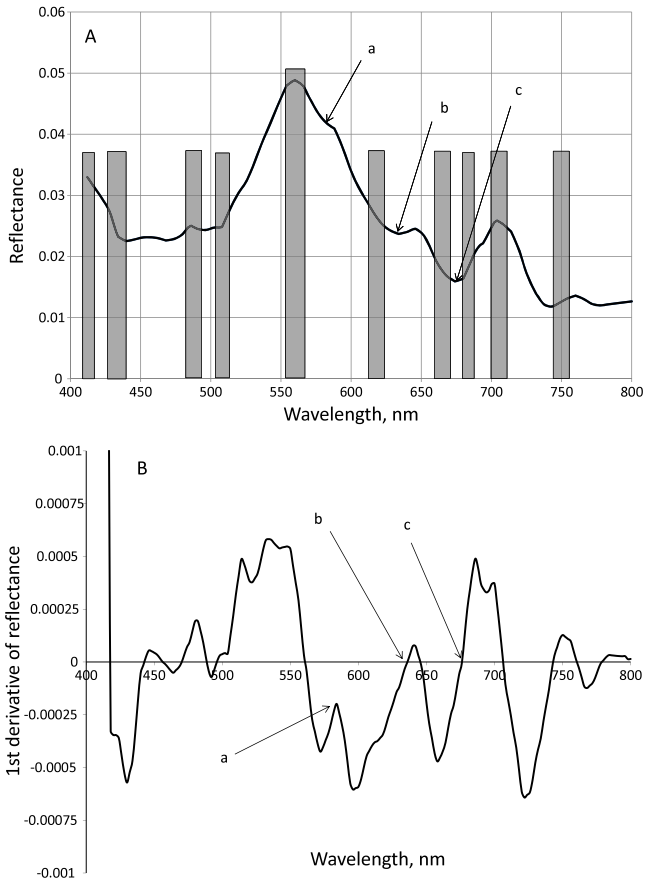

Figure 7. Median reflectance spectrum taken in the Azov Sea with marked locations of spectral bands of MERIS (A) and the first derivative of reflectance (B). Absorption bands of a—phycoerythrin; b—phycocyanin, and c—chlorophyll-a.

Acknowledgments

This research is partially supported by the US Office of Naval Research. Anatoly Gitelson is supported by the University of Nebraska and by a NASA LCLUC program grant NNG06GG17G. Sergey Berdnikov and Vlad Saprygin are UNL collaborators on the NASA funded project. We thank the two anonymous reviewers for helpful and critical comments improving the original manuscript.

References

Bidigare R R, Ondrusek M E, Morrow J H and Kiefer D A 1990 *In vivo* absorption properties of algal pigments *Proc. SPIE* **1302** 290–302

Corson M R and Davis C O 2011 A new view of coastal oceans from the space station *EOS Trans. AGU* **92** 161–2
Dall'Olmo G and Gitelson A A 2005a Effect of bio-optical parameter variability on the remote estimation of chlorophyll-a concentration in turbid productive waters: experimental results *Appl. Opt.* **44** 412–22
Dall'Olmo G and Gitelson A A 2005b *Appl. Opt.* **44** 3342 (erratum)
Dall'Olmo G and Gitelson A A 2006 Effect of bio-optical parameter variability and uncertainties in reflectance measurements on the remote estimation of chlorophyll-a concentration in turbid productive waters: modeling results *Appl. Opt.* **45** 3577–92
Dall'Olmo G, Gitelson A A and Rundquist D C 2003 Towards a unified approach for remote estimation of chlorophyll-a in both terrestrial vegetation and turbid productive waters *Geophys. Res. Lett.* **30** 1038
Darecki M and Stramski D 2004 An evaluation of MODIS and SeaWiFS bio-optical algorithms in the Baltic Sea *Remote Sens. Environ.* **89** 326–50
Gao B-C and Davis C O 1997 Development of a line-by-line-based atmosphere removal algorithm for airborne and spaceborne imaging spectrometers *Proc. SPIE* **3118** 132–41
Gitelson A A 1992 The peak near 700 nm on reflectance spectra of algae and water: relationships of its magnitude and position with chlorophyll concentration *Int. J. Remote Sens.* **13** 3367–73
Gitelson A A, Dall'Olmo G, Moses W, Rundquist D C, Barrow T, Fisher T R, Gurlin D and Holz J 2008 A simple semi-analytical model for remote estimation of chlorophyll-a in turbid waters: validation *Remote Sens. Environ.* **112** 3582–93
Gitelson A A, Gritz U and Merzlyak M N 2003 Relationships between leaf chlorophyll content and spectral reflectance and algorithms for non-destructive chlorophyll assessment in higher plant leaves *J. Plant Physiol.* **160** 271–82
Gitelson A A, Gurlin D, Moses W J and Barrow T 2009 A bio-optical algorithm for the remote estimation of the chlorophyll-a concentration in case 2 waters *Environ. Res. Lett.* **4** 045003
Gitelson A A, Gurlin D, Moses W J and Yacobi Y Z 2011 Remote estimation of chlorophyll-a concentration in inland, estuarine, and coastal waters *Advances in Environmental Remote Sensing, Sensors: Algorithms, and Applications* ed Q Weng (Boca Raton, FL: CRC) pp 449–78
Gitelson A, Keydan G and Shishkin V 1985 Inland waters quality assessment from satellite data in visible range of the spectrum *Sov. Remote Sens.* **6** 28–36
Gitelson A A, Schalles J F and Hladik C M 2007 Remote chlorophyll-a retrieval in turbid, productive estuaries: Chesapeake Bay case study *Remote Sens. Environ.* **109** 464–72
Gitelson A A, Viña A, Ciganda V, Rundquist D C and Arkebauer T J 2005 Remote estimation of canopy chlorophyll content in crops *Geophys. Res. Lett.* **32** L08403
Gons H J 1999 Optical teledetection of chlorophyll a in turbid inland waters *Environ. Sci. Technol.* **33** 1127–32
Gordon H R, Brown J W and Evans R H 1988 Exact Rayleigh scattering calculations for use with the Nimbus 7 Coastal Zone Color Scanner *Appl. Optics.* **27** 862–71
Gordon H R, Brown O B and Jacobs M M 1975 Computed relationships between the inherent and apparent optical properties of a flat homogeneous ocean *Appl. Opt.* **14** 417–27
Gordon H and Morel A 1983 *Remote Assessment of Ocean Color for Interpretation of Satellite Visible Imagery. A Review* (*Springer Lecture Notes on Coastal and Estuarine Studies* vol 4) (Berlin: Springer)
Gower J F R, Doerffer R and Borstad G A 1999 Interpretation of the 685 nm peak in water-leaving radiance spectra in terms of fluorescence, absorption and scattering, and its observation by MERIS *Int. J. Remote Sens.* **20** 1771–86
Lee Z P, Carder K L, Hawes S K, Steward R G, Peacock T G and Davis C O 1994 Model for the interpretation of hyper-spectral remote-sensing reflectance *Appl. Opt.* **33** 5721–32
Lucke R L, Corson M, McGlothlin N R, Butcher S D, Wood D L, Korwan D R, Li R R, Snyder W A, Davis C O and Chen D T 2011 The Hyperspectral Imager for the Coastal Ocean: instrument description and first images *Appl. Opt.* **50** 1501–16
Matishov G G, Povazhnyi V V, Berdnikov S V, Moses W J and Gitelson A A 2010 Satellite estimation of chlorophyll-a concentration and phytoplankton primary production in the Sea of Azov *Proc. Russ. Acad. Sci., Biol. Sci.* **432** 216–9
Morel A and Prieur L 1977 Analysis of variations in ocean color *Limnol. Oceanogr.* **22** 709–22
Moses W J, Gitelson A A, Berdnikov S and Povazhnyy V 2009a Estimation of chlorophyll-a concentration in case II waters using MODIS and MERIS data-successes and challenges *Environ. Res. Lett.* **4** 045005
Moses W J, Gitelson A A, Berdnikov S and Povazhnyy V 2009b Satellite estimation of chlorophyll-a concentration using the red and NIR bands of MERIS—the Azov Sea case study *IEEE Geosci. Remote Sens. Lett.* **6** 845–9
O'Reilly J, Maritorena S, Mitchell B, Siegel D, Carder K, Garver S, Kahru M and McClain C 1998 Ocean color chlorophyll algorithms for SeaWiFS *J. Geophys. Res.* **103** 24397–954
O'Reilly J *et al* 2000 SeaWiFS Postlaunch Calibration and Validation Analyses, Part 3 *NASA Tech. Memo.* 2000-206892, vol 11, ed S Hooker and E Firestone (Greenbelt, MD: NASA Goddard Space Flight Center) p 49
Schalles J F 2006 Optical remote sensing techniques to estimate phytoplankton chlorophyll a concentrations in coastal waters with varying suspended matter and CDOM concentrations *Remote Sensing of Aquatic Coastal Ecosystem Processes: Science and Management Applications* ed L Richardson and E Ledrew (Berlin: Springer) pp 27–79
Simis S G H, Peters S W M and Gons H J 2005 Remote sensing of the cyanobacterial pigment phycocyanin in turbid inland water *Limnol. Oceanogr.* **50** 237–45
Simis S G H, Tijdens M, Hoogveld H L and Gons H J 2007 Optical signatures of the filamentous cyanobacterium Leptolyngbya boryana during mass viral lysis *Limnol. Oceanogr.* **52** 184–97
Stumpf R P and Tyler M A 1988 Satellite detection of bloom and pigment distributions in estuaries *Remote Sens. Environ.* **24** 385–404
Vasilkov A and Kopelevich O 1982 Reasons for the appearance of the maximum near 700 nm in the radiance spectrum emitted by the ocean layer *Oceanology* **22** 697–701
Yacobi Y Z, Moses W J, Kaganovsky S, Sulimani B, Leavitt B C and Gitelson A A 2011 NIR-red reflectance-based algorithms for chlorophyll-a estimation in mesotrophic inland and coastal waters: Lake Kinneret case study *Water Res.* **45** 2428–36